Structure and Properties of a New Electride, Rb^+(cryptand[2.2.2])e^-

Qingshan Xie, Rui H. Huang, Andrew S. Ichimura, Richard C. Phillips, William P. Pratt, Jr.,† and James L. Dye*

Contribution from the Departments of Chemistry and Physics/Astronomy and Center for Fundamental Materials Research, Michigan State University, East Lansing, Michigan 48824-1322

Received December 13, 1999

Abstract: This is the sixth electride whose crystal structure has been determined and the fourth to show polymorphism. Crystals of the title electride prepared from mixed solvents have a structure similar to that of Li^+(cryptand[2.1.1])e^-. Electrons occupy cavities that are connected by "ladder-like" channels. The static and spin magnetic susceptibilities of polycrystalline samples that contain this polymorph (called phase α) show Heisenberg 1D antiferromagnetic behavior with $-J/k_B = 30$ K. Similar to other electrides with "localized" electrons, this electride is a poor conductor ($\sigma < 10^{-4}$ ohm^{-1}cm^{-1}). Thin films prepared by high vacuum co-deposition of Rb metal and cryptand[2.2.2] have optical spectra and near-metallic electrical conductivity nearly identical with those of K^+(cryptand[2.2.2])e^-. These properties would not be expected if the film structure were the same as that obtained for crystals. Rather, they suggest that the films consist of microcrystals whose structure is similar to that of K^+(cryptand[2.2.2])e^-. Polycrystalline samples prepared by slow evaporation of methylamine from stoichiometric solutions at −78 °C (called phase β) have properties similar to those of K^+(cryptand[2.2.2])e^-. The conductivity of samples that contain phase β is more than an order of magnitude larger than those with phase α. Magnetic and spin susceptibilities show that phase β samples have much larger electron−electron interactions. As with K^+(cryptand[2.2.2])e^-, the magnetic susceptibility of phase β is compatible with alternating linear chain Heisenberg antiferromagnetism, with $-J/k_B \approx 300$ K and $-J'/k_B \approx 240$ K. Thin vapor co-deposited films show abrupt changes in the conductivity and optical spectrum at −12 °C that suggest a transition that may be conversion of phase β to phase α.

Introduction

Electrides are crystalline ionic compounds in which trapped electrons serve as the counterions to complexed alkali metal cations.[1−10] Although the synthesis of powdered electrides is straightforward, it has been very difficult to obtain single crystals suitable for structure determination by X-ray diffraction. While we have determined the crystal structures of more than 40 *alkalides*,[11−20] prior to this work only five electride structures had been determined in a 13 year period.[21−28] There are at least three reasons for this difficulty: (1) Electrides are even more thermally unstable than alkalides, as are the precursor solutions that contain the solvated electron. (2) Except with lithium, alkali metal anions, M^-, tend to cocrystallize with electrides, leading to crystalline disorder. (3) Three of the five previously studied electrides exhibit polymorphism, with a tendency for one of the phases in each case to be disordered.[25,28−30]Thus, while

† Department of Physics/Astronomy.

(1) Dye, J. L.; Ellaboudy, A. *Chem. Br.* **1984**, *20*, 210−215.
(2) Dye, J. L. *Prog. Inorg. Chem.* **1984**, *32*, 327−441.
(3) Dye, J. L. *Sci. Am.* **1987**, *257*, 66−75.
(4) Dye, J. L. *Science* **1990**, *247*, 663−668.
(5) Dye, J. L.; Huang, R. H. *Chem. Br.* **1990**, *26*, 239−244.
(6) Dye, J. L. *Nature* **1993**, *365*, 10−11.
(7) Wagner, M. J.; Dye, J. L. *Annu. Rev. Mater. Sci.* **1993**, *23*, 223−253.
(8) Dye, J. L.; Wagner, M. J.; Overney, G.; Huang, R. H.; Nagy, T. F.; Tomanek, D. *J. Am. Chem. Soc.* **1996**, *118*, 7329−7336.
(9) Wagner, M. J.; Dye, J. L. In *Molecular Recognition: Receptors for Cationic Guests*, 1st ed.; Gokel, G. W., Ed.; Pergamon Press: Oxford, U.K., 1996; Vol. 1, pp 477−510.
(10) Dye, J. L. *Inorg. Chem.* **1997**, *36*, 3816−3826.
(11) Tehan, F. J.; Barnett, B. L.; Dye, J. L. *J. Am. Chem. Soc.* **1974**, *96*, 7203−7208.
(12) Huang, R. H.; Ward, D. L.; Kuchenmeister, M. E.; Dye, J. L. *J. Am. Chem. Soc.* **1987**, *109*, 5561−5563.
(13) Dawes, S. B.; Ward, D. L.; Fussa-Rydel, O.; Huang, R.-H.; Dye, J. L. *Inorg. Chem.* **1989**, *28*, 2132−2136.
(14) Kuchenmeister, M. E.; Dye, J. L. *J. Am. Chem. Soc.* **1989**, *111*, 935−938.
(15) Huang, R. H.; Ward, D. L.; Dye, J. L. *J. Am. Chem. Soc.* **1989**, *111*, 5707−5708.
(16) Ward, D. L.; Huang, R. H.; Dye, J. L. *Acta Crystallogr.* **1990**, *C46*, 1838−1841.
(17) Ward, D. L.; Huang, R. H.; Dye, J. L. *Acta Crystallogr.* **1990**, *C46*, 1833−1835.
(18) Huang, R. H.; Ward, D. L.; Dye, J. L. *Acta Crystallogr.* **1990**, *C46*, 1835−1837.
(19) Huang, S. Ph.D. Dissertation, Michigan State University, 1994.
(20) Huang, R. H.; Huang, S. Z.; Dye, J. L. *J. Coord. Chem.* **1998**, *46*, 13−31.
(21) Dawes, S. B.; Ward, D. L.; Huang, R. H.; Dye, J. L. *J. Am. Chem. Soc.* **1986**, *108*, 3534−3535.
(22) Huang, R. H.; Faber, M. K.; Moeggenborg, K. J.; Ward, D. L.; Dye, J. L. *Nature* **1988**, *331*, 599−601.
(23) Ward, D. L.; Huang, R. H.; Dye, J. L. *Acta Crystallogr.* **1988**, *C44*, 1374−1376.
(24) Ward, D. L.; Huang, R. H.; Kuchenmeister, M. E.; Dye, J. L. *Acta Crystallogr.* **1990**, *C46*, 1831−1833.
(25) Dawes, S. B.; Eglin, J. L.; Moeggenborg, K. J.; Kim, J.; Dye, J. L. *J. Am. Chem. Soc.* **1991**, *113*, 1605−1609.
(26) Wagner, M. J.; Huang, R. H.; Eglin, J. L.; Dye, J. L. *Nature* **1994**, *368*, 726−729.
(27) Wagner, M. J.; Dye, J. L. *J. Solid State Chem.* **1995**, *117*, 309−317.
(28) Huang, R. H.; Wagner, M. J.; Gilbert, D. J.; Reidy-Cedergren, K. A.; Ward, D. L.; Faber, M. K.; Dye, J. L. *J. Am. Chem. Soc.* **1997**, *119*, 3765−3772.
(29) Wagner, M. J.; Huang, R. H.; Dye, J. L. *J. Phys. Chem.* **1993**, *97*, 3982−3984.
(30) Wagner, M. J.; Ichimura, A. S.; Huang, R. H.; Phillips, R. C.; Dye, J. L. *J. Phys. Chem. B* **2000**, *104*, 1078−1087.

10.1021/ja9943445 CCC: $19.00
Published on Web 07/07/2000

electride powders are relatively easy to prepare and were studied as early as 1981,[31] correlation of structure and properties could only be made for a few electrides.

Both experiment[6,8,10] and theory[32,33] show that the electron released by the process

$$M(s) + nL \rightleftarrows M^+(L)_n + e^- \quad (1)$$

occupies the anion vacancy (cavity) created by close-packing of the large complexed cation, $M^+(L)_n$. Electrons in adjacent cavities interact to an extent that is related to the size(s) of the connecting channel(s).[10] In the crystalline electrides synthesized to date, L is either 18-crown-6 (18C6) or 15-crown-5 (15C5) with $n = 2$ (sandwich cation) or cryptand[2.2.2] (C222) or cryptand[2.1.1] (C211) with $n = 1$. Except for the complicated mixed crown−ether electride, $[Cs^+(18C6)(15C5)e^-]_6 \cdot 18C6$, all crystalline electrides may be viewed to first order as linear chain Heisenberg antiferromagnets (LCHA) with the coupling constant $-J/k_B$ ranging from 3 K for $Cs^+(15C5)_2e^-$ to 430 K for $K^+(C222)e^-$. The latter electride has strong coupling to both nearest- and next-nearest-neighbor electrons and follows the alternating linear chain Heisenberg antiferromagnet (ALCHA) model.[34] This behavior is in complete accord with the cavity-channel structure of $K^+(C222)e^-$, which has a *pair* of electrons in a dumbell-shaped cavity and large channels that connect adjacent cavities.[8,22] Since the penetration of electron density into the region occupied by the complexed cation is minimized by the Pauli Exclusion principle, the electrons in crystalline electrides may be considered to form well-defined "electron lattice gases" with weak to moderate inter-electron coupling.

We report in this paper the synthesis, structure, and properties of a crystalline phase of $Rb^+(C222)e^-$, a new electride with a completely unexpected structure. Since the structures of $K^+(C222)e^-$, $K^+(C222)K^-$, and $Rb^+(C222)Rb^-$ are similar to one another, with *pairs* of anions (including e^-) trapped in dumbbell-shaped cavities,[15,16,22] we expected the structure of $Rb^+(C222)e^-$ to be similar. The only change would be the replacement of Rb^- by e^-. This preconception was reinforced by the extensive studies of co-deposited thin films of $Rb^+(C222)e^-$ reported in this paper. Films of stoichiometry $Rb^+(C222)e^-$ have optical spectra and conductivities that are virtually identical with those of $K^+(C222)e^-$ films.[35] As described in this paper, however, the crystal structure and properties of a phase of $Rb^+(C222)e^-$ that was prepared by slow crystallization from mixed solvents are very different from those expected on the basis of the film studies. On the other hand, powder samples formed by slow evaporation of methylamine from a stoichiometric solution have magnetic and spin susceptibilities that mimic those of $K^+(C222)e^-$. These results strongly indicate that $Rb^+(C222)e^-$, as is the case for three other electrides, exists in at least two different forms.

Experimental Section

Solvent, complexant and metal sources and purification, manipulation of solutions, and transfer of crystals or powdered samples into glass tubes for seal-off have been described in detail elsewhere.[2,9,36] All syntheses were carried out by vacuum-line methods, with introduction of the complexant and metal into specially cleaned borosilicate "K-cells" in a helium-filled glovebox as previously described.

As for other electrides, the synthesis methodology is simple *in principle*. Just dissolve Rb metal in a solvent such as methylamine ($MeNH_2$) in the presence of an equivalent amount of C222. Then add a less polar cosolvent such as trimethylamine (Me_3N) or diethyl ether (Et_2O) and grow crystals by slowly cooling the solution or slowly removing methylamine by preferential solvent vaporization. While powdered samples of stoichiometry $Rb^+(C222)e^-$ can be made by simply evaporating $MeNH_2$ from the stoichiometric solution (see later), crystal growth from mixed solvents was plagued with difficulties. Regardless of the cosolvent used, even when it is completely miscible with $MeNH_2$ in the absence of solute, solutions of $Rb^+(C222)e^-$ separated into two liquid phases, a small amount of a concentrated, viscous blue-black solution that tended to stick to the walls as droplets, and a more fluid deep blue solution. Over a dozen separate attempts were made to circumvent these problems without success.

The more concentrated solution remained behind when the more dilute solution was poured into a separate compartment. A few small crystals were grown from the more dilute solution by slowly decreasing the temperature from −40 to −75 °C with two subsequent cycles from −60 to −75 °C and −65 to −75 °C. The entire process took about 40 h. It was necessary to cycle the temperature in this way to obtain crystals large enough for structure determination. The crystals were washed with cold diethyl ether and evacuated for several hours to $\sim 10^{-5}$ Torr. At no point was the temperature allowed to exceed −40 °C. Very small yields (only a few milligrams) of tiny crystals were obtained in three separate runs.

The shiny black crystals of $Rb^+(C222)e^-$ were kept under vacuum in the K-cell at −78 °C and transferred in a nitrogen-filled glovebag into a depression in a cold copper block (kept at −60 °C) and covered with cold purified octane.[13,23] Microscopic examination was used to select a suitable crystal that was then picked up with a glass fiber with vacuum grease on its tip and transferred to the diffractometer in a cold N_2 gas stream (−60 °C). X-ray data were collected at −90 °C with a Siemens P3 diffractometer equipped with a low-temperature accessory.

Because the yield of crystals was too small for the study of properties other than the structure, polycrystalline (powder) samples that contain $Rb^+(C222)e^-$ (but not exclusively) were prepared by slow evaporation of the mixed solvents from the more concentrated solution, followed by prolonged evacuation at $\sim 10^{-5}$ Torr to remove all solvent. This method is fraught with difficulties since solutions in the mixed solvents undoubtedly contain other species than $Rb^+(C222)$ and e^-_{solv}. As one moves from methylamine to a less polar solvent such as trimethylamine or diethyl ether, the equilibrium

$$Rb^+(C222) + 2e^-_{solv} \rightleftarrows Rb^- + C222 \quad (2)$$

shifts to the right. As the mixed solvent evaporates, the fraction of less polar (and less volatile) solvent increases. The result is that the residue from evaporation contains not only $Rb^+(C222)e^-$ but also $Rb^+(C222)Rb^-$ and C222, as well as any decomposition products.

As described later, simple, slow evaporation of methylamine from a stoichiometric solution, followed by prolonged evacuation, produces powders with very different properties than those obtained from mixed solvents. To distinguish between the two kinds of powder samples, we refer to those obtained from mixed solvents as *phase* α while those obtained from methylamine alone are designated *phase* β. The properties clearly indicate that phase α contains crystallites with the known structure described above, while phase β is dominated by a different form of $Rb^+(C222)e^-$. The properties of the latter polymorph suggest that its structure is similar to the common geometry of $K^+(C222)e^-$, $K^+(C222)K^-$, and $Rb^+(C222)Rb^-$. Despite numerous attempts with different conditions, we were unable to prepare crystals of phase β suitable for structure determination. The need to maintain low temperatures with the rigorous exclusion of air, the lack of suitable equipment, and the ubiquitous formation of mixed phases prevented us from obtaining powder X-ray diffraction patterns of either phase α or phase β. While EPR spectra could, in principle, have been obtained

(31) Landers, J. S. Ph.D. Dissertation, Michigan State University, East Lansing, MI, 1981.
(32) Allan, G.; DeBacker, M. G.; Lannoo, M.; Lefebvre, J. *Europhys. Lett.* **1990**, *11*, 49−53.
(33) Singh, D. J.; Krakauer, H.; Haas, C.; Pickett, W. E. *Nature* **1993**, *365*, 39−42.
(34) Hall, J. W.; Marsh, W. E.; Weller, R. R.; Hatfield, W. E. *Inorg. Chem.* **1981**, *20*, 1033−1037.
(35) Hendrickson, J. E.; Pratt, W. P., Jr.; Phillips, R. C.; Dye, J. L. *J. Phys. Chem. B* **1998**, *102*, 3917−3926.
(36) Dye, J. L. *J. Phys. Chem.* **1984**, *88*, 3842−3846.

on the tiny single crystals, attempts to transfer them into EPR tubes were frustrated by their adherence to the walls and their tendency to shatter.

After evacuation to $\sim 10^{-5}$ Torr for several hours, both types of powder sample were transferred into glass tubes attached to the K-cell and sealed-off under vacuum at −78 °C. Samples were stored at liquid nitrogen temperatures prior to use and transferred while cold into the appropriate pre-cooled equipment in a nitrogen-filled glovebag.

Thin films (2200−4200 Å thick) of stoichiometry Rb C222 were prepared on a cold sapphire substrate by high-vacuum co-deposition of Rb and C222. The method was similar to that used for the study of Na-C222 and K-C222 films.[35,37−40] Optical absorbance and four-probe conductivities were obtained as previously described.[35] Substrate temperatures during deposition were maintained constant and ranged from −40 to −70 °C for various runs. The temperature dependence of the optical spectrum and the conductivity were measured and thermal decomposition was monitored by the decrease in peak absorbance and/or the oscillator strength. Decomposed films show no absorption peaks in the visible or near-IR regions. The overall stoichiometry of the film was controlled by measuring the deposition rate of the metal and the complexant with separate thickness monitors and by controlling the respective oven temperatures. Generally the *overall* metal-to-complexant ratio could be controlled to within ± 5% although somewhat greater rate deviations occurred during deposition.

EPR spectra of powder samples were obtained with a Bruker ESP300E spectrometer (X-band, 9.5 GHz). Temperature control between 4 and 250 K was maintained with an Oxford Instruments 9000 liquid helium cryostat. A Bruker ER035M NMR gaussmeter and an EIP model 25B frequency counter were used to obtain accurate *g*-values. The intensities were determined by double integration of the EPR spectra after subtracting a constant background correction. Magnetic susceptibilities of powders were measured with a Quantum Design MPMS2 SQUID magnetometer. The diamagnetic contributions from the sample and holder were obtained by allowing the sample to decompose in the magnetometer by simply raising the temperature to 300 K.

Differential scanning calorimetry (DSC) used a Shimadzu DSC-50 calorimeter with a low-temperature attachment. Powder samples were hermetically sealed in aluminum pans with a liquid nitrogen-cooled press in a nitrogen-filled glovebag that also enclosed the calorimeter. The sample holder was pre-cooled to 130 K prior to loading and was protected against moisture condensation by a steady flow of helium gas prior to and during the measurements. Two-probe powder conductivities and impedance spectra were obtained as previously described.[41]

Results and Discussion

Crystal Structure. Phase α of Rb^+(C222)e^- crystallized in the $P\bar{1}$ space group (No. 2). The crystal data are given in Table 1 and Figure 1 displays the structure of the Rb^+(C222) unit. Although the space group is different, the cavity-channel geometry is similar to that of Li^+(C211)e^-.[28] As shown in Figure 2, the dominant void-space geometry consists of parallel zigzag chains of cavities and large channels along the *a*-direction. Each cavity is large enough to contain a hard sphere of diameter 3.9 Å, while a sphere of diameter 2.6 Å could move through the major channel. Note that the surfaces shown in Figure 2 represent the locus of points 0.65 Å from the atomic van der Waals surfaces.[8] As a result, they do not show channels with diameters smaller than 1.3 Å. However, as shown in Figure 3 for a distance of 0.45 Å, such channels do exist. The major zigzag features along *a* are connected at the "corners" by smaller channels (B) of diameter 1.15 Å to form "ladder-like" 1D chains along *a*. Adjacent chains are connected along *b* by channels (C) of diameter 1.04 Å and (nearly) along *c* by 0.72 Å diameter

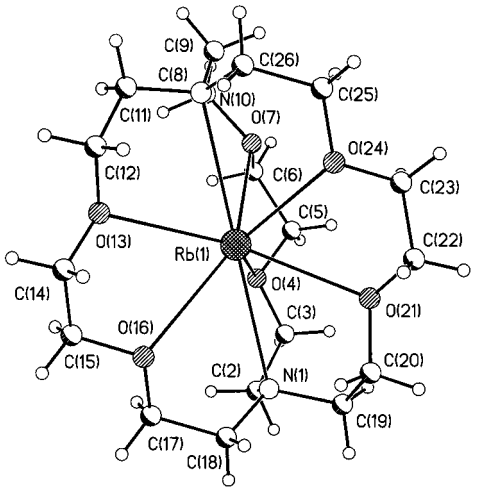

Figure 1. Ortep diagram of the Rb^+(C222) unit in Rb^+(C222)e^-.

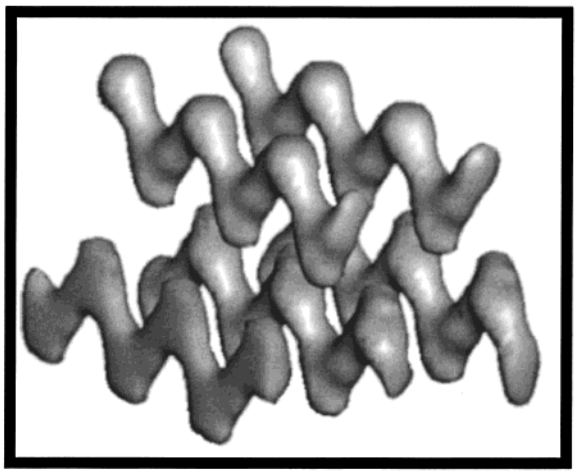

Figure 2. Perspective view of the dominant cavity-channel geometry of the α phase of Rb^+(C222)e^-. The zigzag chains are along the *a*-direction. The surfaces shown encompass void spaces that lie 0.65 Å from the atomic van der Waals surfaces.

Table 1. Crystallographic and Refinement Data for Rb^+(C222)·e^-

space group	triclinic, $P\bar{1}$
cell parameters	
a, Å	8.7297(38)
b, Å	11.5653(66)
c, Å	13.9468(69)
α, deg	64.195(4)
β, deg	71.931(36)
γ, deg	84.744(41)
Z	2
crystal dimensions, mm	0.1 × 0.1 × 0.2
scan type	*ω*
max 2*θ*, deg	50
temp (K)	200
no. of reflcns collected	2468
no. of unique reflcns	2268
no. of reflcns used in refinement with $F_o^2 > 3\sigma(F_o^2)$	1633
no. of variables	307
R	0.145
high peak in final diffraction map, e/Å^3	0.18

(37) Skowyra, J. B.; Dye, J. L.; Pratt, W. P., Jr. *Rev. Sci. Instrum.* **1989**, *60*, 2666−2672.
(38) Hendrickson, J. E. Ph.D. Dissertation, Michigan State University, East Lansing, Michigan, 1994.
(39) Hendrickson, J. E.; Kuo, C. T.; Xie, Q.; Pratt, W. P., Jr.; Dye, J. L. *J. Phys. Chem.* **1996**, *100*, 3395−3401.
(40) Hendrickson, J. E.; Xu, G.; Pratt, W. P., Jr.; Dye, J. L. *J. Phys. Chem. A* **1997**, *101*, 4149−4155.
(41) Moeggenborg, K. J.; Papaioannou, J.; Dye, J. L. *Chem. Mater.* **1991**, *3*, 514−520.

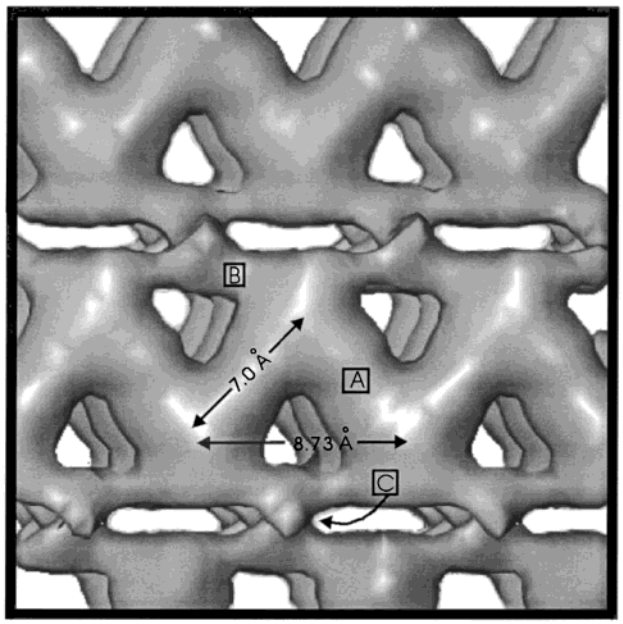

Figure 3. Geometry of the void spaces at 0.45 Å from the atomic van der Waals surfaces of the α phase of $Rb^+(C222)e^-$. This shows the "ladder-like" chain of cavities and channels, A and B, along the *a*-direction (horizontal). Connections along *b* (nearly perpendicular to the plane of the figure) between chains are by smaller channels, labeled C. The *c*-axis is in the plane of the figure at an angle of 72° to the horizontal.

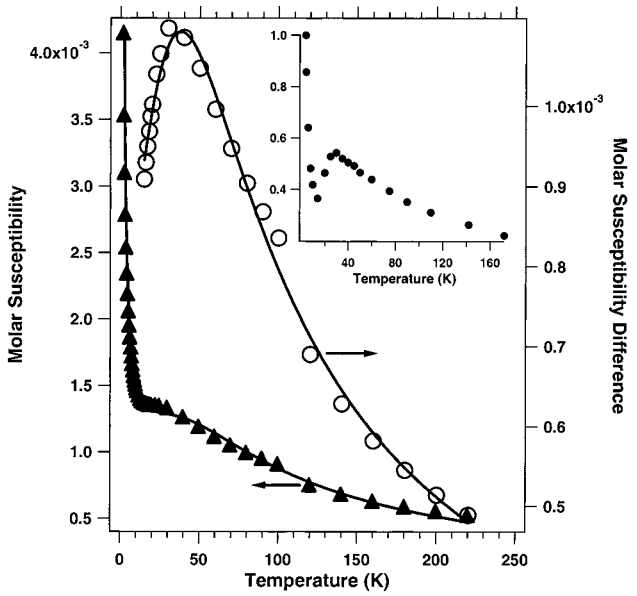

Figure 4. Magnetic susceptibility of phase α powders of $Rb^+(C222)e^-$ as a function of temperature. Triangles give the total molar susceptibility, (left axis) while circles give the susceptibility after subtraction of a "Curie tail" (right axis). Solid lines are the best fit of the LCHA model to the data and include a small contribution from phase *β*. (The solid line through the triangles also includes a Curie law term.) The inset shows the relative EPR spin susceptibility of a phase α sample.

channels (not developed in the view of Figure 3). Thus, the void spaces in the crystal form a 3D network of cavities and channels. But the feature that dominates the inter-electron coupling is the very open 1D zigzag chain in which electron trapping sites are 7.0 Å apart, connected by channels (A) of diameter 2.6 Å. No crystals of phase *β* were obtained, but the properties of powders obtained by evaporation of methylamine from stoichiometric solutions suggest a very different and more open cavity-channel geometry.

Magnetic Properties of Phase α. Despite the complications caused by the presence of other species than the electride in phase α, it was important to determine whether the behavior of polycrystalline powders is that expected from the crystal structure. The most sensitive indicator of the cavity-channel geometry of crystalline electrides is the magnetic susceptibility. For example, the crystalline phases of $Cs^+(18C6)_2e^-$ and $Cs^+(15C5)_2e^-$ each show a peak in the magnetic susceptibility at 50 and 5 K respectively, while disordered phases of these electrides show only Curie−Weiss behavior.[25,29] Similarly, the two forms of $Li^+(C211)e^-$ have susceptibility peaks at 65 K for crystalline samples and at 20 K for (apparently disordered) powder samples.[28] The four crystalline electrides with primarily 1D channel structures have coupling constants that correlate very well with the sizes of the major channels.[10] Therefore, magnetic susceptibilities can be used to infer structural information.

To determine whether polycrystalline α phase samples of $Rb^+(C222)e^-$ have the susceptibility expected from the crystal structure, we measured the static susceptibilities of three different preparations and the EPR spin susceptibility of one of them as functions of temperature. All showed the same general behavior. Figure 4 shows that the molar susceptibility has a maximum at ∼30 K, after subtraction of a "Curie Law tail" of the form aC/T, in which a is the fraction of "defect electrons" (0.0185 ± 0.0003 in this case) and C is the Curie constant (0.376 for $S = {}^1/_2$). The spin susceptibility, shown in the inset to Figure 4, shows clearly the maximum in the susceptibility as well as the Curie tail. The static susceptibility data above 15 K can be fit approximately by the LCHA model with $-J/k_B = 30.7 \pm 0.5$ K. The function used is given in ref 10. It should be noted that the LCHA contribution to the susceptibility of this sample accounts for only (30.6 ± 0.1)% of the expected total spin concentration. The remainder is largely diamagnetic and probably consists primarily of free C222, $Rb^+(C222)Rb^-$, and decomposition products. It is also likely that these samples contain some phase *β* powders. Indeed, the inclusion of (16 ± 4)% of phase *β* improved the fit of the susceptibility data without substantially changing the amount of phase α ((29.1 ± 0.5)%) or the value of $-J/k_B$ (28.7 ± 0.5 K). The solid lines in Figure 4 show the fit of the data. Until large enough samples of the pure crystalline phase can be obtained, we can only be sure that magnetic susceptibility of the powder referred to as phase α is dominated by crystallites with the known crystal structure.

Assuming that the magnetic susceptibility of phase α reflects the behavior of crystals with the known structure, the previous correlation between the coupling constant and the cross-sectional area of the major channel[10] has been extended to include both the new electride $Rb^+(C222)e^-$ and the additional new crystalline electride $K^+(15C5)_2e^-$. (The latter electride will be described in a separate publication.) The result, shown in Figure 5, extends the correlation from four to six electrides. This provides further support for a model in which the extent of electronic wave function overlap within the 1D channels determines the magnitude of the coupling constant. A challenge to theorists is to calculate from quantum theory the coupling constant as a function of the size and shape of the cavity and the length and area of the connecting channels. The good correlation between the coupling constant and the size of the channel, compared with other electrides, provides strong evidence that the powder obtained by mixed solvent evaporation does indeed contain crystals with the known structure.

Powder Conductivities. The two-probe dc conductivity of polycrystalline phase α samples was nearly independent of temperature between 120 and 250 K. The average specific

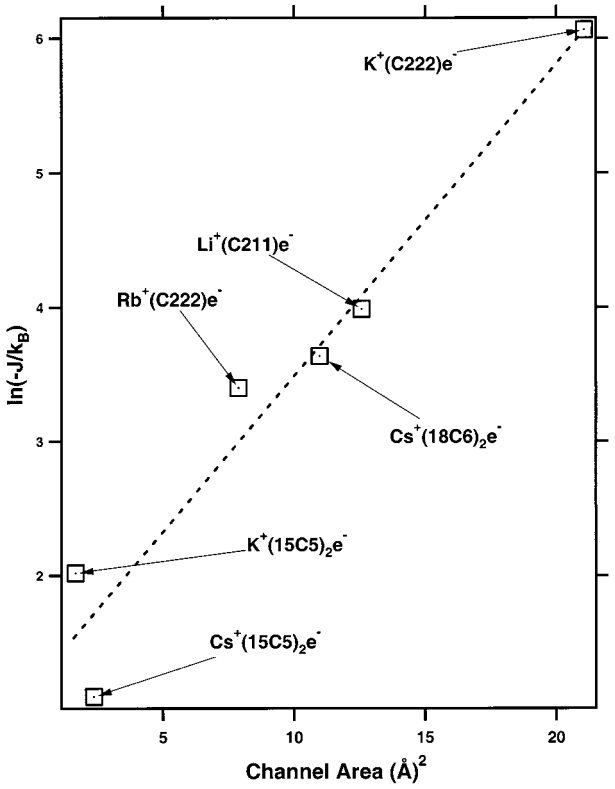

Figure 5. Relation of the primary coupling constant of six electrides to the cross-sectional area of the channels that connect the electron-trapping sites. In all cases except $K^+(C222)e^-$ the data were fit by a 1D Heisenberg (LCHA) model. The data for $K^+(C222)e^-$ were fit by the 1D (ALCHA) model that includes both nearest-neighbor and next-nearest-neighbor interactions.

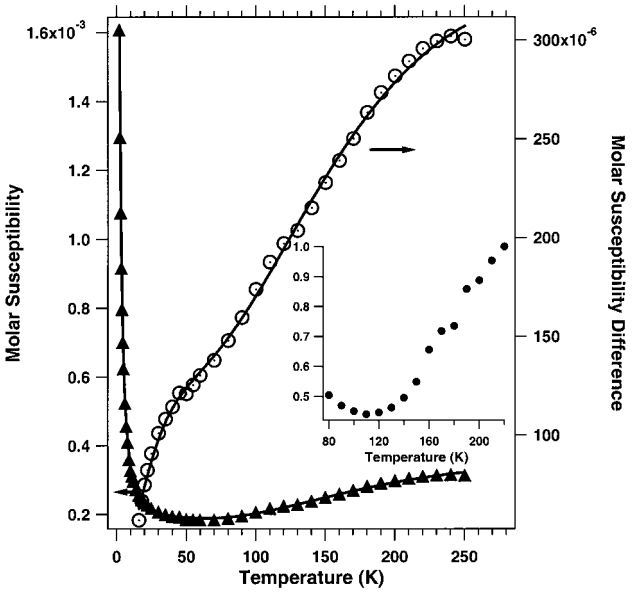

Figure 6. Magnetic susceptibility of phase β powders of $Rb^+(C222)e^-$ as a function of temperature. Triangles give the total molar susceptibility (left axis) while circles give the susceptibility after subtraction of a "Curie tail" (right axis). Solid lines are the best fit of the ALCHA model to the data and include a small contribution from phase α. (The solid line through the triangles also includes a Curie law term.) The inset shows the relative EPR spin susceptibility of a phase β sample.

conductance was 5×10^{-5} ohm^{-1} cm^{-1} with an apparent activation energy of only 0.0013 eV. At 260 K the specific conductance dropped abruptly to $<10^{-10}$ ohm^{-1} cm^{-1}, probably because of decomposition. Irreversible reduction of the cryptand to the expected products, a glycolate and ethylene, would yield an insulating sample.[42] The low conductivity of the crystalline phase is expected from the structure. All other electrides except $K^+(C222)e^-$ are highly resistive[10,41] (see Figure 10 of ref 10 for example). In the case of $K^+(C222)e^-$, both polycrystalline samples and thin films have nearly metallic conductivities.

To minimize the resistance due to a Schottky barrier at the electrode−sample interface, the electrodes were coated with rubidium metal in a helium-filled glovebox prior to loading the cell with a cold sample in a nitrogen-filled glovebag.[41] In addition to two-probe dc conductivities, extensive measurements were made by impedance spectroscopy with frequencies between 5 Hz and 13 MHz. The zero frequency intercept was 1×10^{-4} ohm^{-1} cm^{-1} at 110 K and reached a maximum of 1.6×10^{-3} ohm^{-1} cm^{-1} at 160 K.

Unlike magnetic susceptibilities, the conductivity is expected to be strongly influenced by the presence of impurities. Thus, we can only conclude that the crystalline phase of $Rb^+(C222)e^-$, like other electrides with relatively small inter-cavity channels, is a poor conductor.

Properties of Phase β Powders. The conductivities of powders formed by slow evaporation of methylamine alone (phase β) were consistently greater than those of phase α, as found by both two-probe dc measurements and impedance spectroscopy. Between 110 and 160 K the complex impedance of samples with rubidium-coated electrodes was nearly independent of the applied voltage from 0.02 to 1.00 V, with an average total decrease in the zero frequency intercept of 6%. Over this temperature range the specific conductance increased from 0.017 ohm^{-1} cm^{-1} at 110 K to 0.042 ohm^{-1} cm^{-1} at 160 K, with an apparent activation energy of 0.030 eV.

Although the conductivity of phase β is more than an order of magnitude higher than that of phase α, it is still more than 2 orders of magnitude lower than that of vapor co-deposited films (see below). Since, as with $K^+(C222)e^-$, the resistivity may be dominated by electrode and grain boundary effects, and indeed may be defect conductivity, it is difficult to compare the results from different samples.

The larger conductivity of powders formed by evaporation of methylamine from stoichiometric solutions in pure methylamine suggested that they contain another phase (β) with a structure that is different from that of crystalline phase α. This view is strongly supported by comparison of their magnetic susceptibilities. As shown in Figure 6, both the static and spin susceptibilities of phase β powders are entirely different from those obtained with phase α powders (Figure 4). For a β phase sample, subtraction of a "Curie tail" that corresponds to only 0.84% spins leaves a paramagnetic susceptibility that increases gradually with increasing temperature (Figure 6). The spin susceptibility obtained from EPR measurements also shows this behavior. The resemblance to the temperature dependence of the susceptibility of $K^+(C222)e^-$ is striking.[22,43] In that case, the crystal structure indicates that the coupling between spins that form the electron pair (in the dumbell-shaped cavity) should be strong. The very wide channel that connects adjacent cavities suggests that next-nearest-neighbor interactions should also be strong. The one-dimensional nature of the cavity-channel system implies that the Heisenberg ALCHA model should be applicable. The measured susceptibilities of $K^+(C222)e^-$ are in excellent agreement with this assumption, although the electride decom-

(42) Cauliez, P. M.; Jackson, J. E.; Dye, J. L. *Tetrahedron Lett.* **1991**, *32*, 5039−5042.

(43) Wagner, M. J. Ph.D. Dissertation, Michigan State University, 1994.

poses before a maximum in the susceptibility can be reached. The similarity of the magnetic susceptibility behavior of phase β powders of $Rb^+(C222)e^-$ to that of $K^+(C222)e^-$ suggests similar cavity-channel geometries.

The susceptibility above 130 K can be reasonably well fit by numerical expressions for the ALCHA model.[34,43] This gives (79 ± 8)% spins, a primary coupling constant, $-J/k_B$, of 295 ± 19 K, and a coupling constant to next-nearest-neighbor electrons, $-J'/k_B$, of 240 ± 10 K. Without the comparison to the behavior of $K^+(C222)e^-$, the limited temperature range would make such a fit questionable. But we can at least conclude that the temperature dependence of the susceptibility is very different from that of phase α and that it is consistent with the ALCHA model used for $K^+(C222)e^-$.[43]

The readily apparent shoulder at 30−50 K in the difference susceptibility shown in Figure 6 suggests the presence of "contamination" by phase α. Because of the smaller coupling constant for this phase, even minor amounts would have a pronounced effect on the susceptibility. By using the parameters determined above for phase α and adjusting the amounts of phases α and β and the two coupling constants of phase α, the overall fits to the data shown by the solid lines in Figure 6 were obtained. The parameters correspond to (5.1 ± 0.2)% of phase α, (61 ± 2)% of phase β, $-J/k_B = 303 \pm 7$ K, and $-J'/k_B = 139 \pm 2$ K. There are too many parameters and they are too strongly coupled to one another to yield reliable values of J, and particularly J', but again, the susceptibility is compatible with the model used. As a result, we conclude that phase β of $Rb^+(C222)e^-$ might well have a cavity-channel geometry that is similar to that of the potassium-based electride.

Thermal Decomposition. DSC studies of both α and β powders demonstrated the thermal instability of this electride. Exothermic decomposition began at ca. −5 °C at a heating rate of 10 deg min^{-1} and was complete by 20 °C. Such instability requires that, as with other electrides, all operations from the initial synthesis to the study of properties be carried out at reduced temperatures.

Thin Films. An extensive study of films of $K^+(C222)e^-$ and $K^+(C222)K^-$ produced by high-vacuum co-deposition of potassium and C222 has been published.[35] The optical and conductivity behavior of these films has been reliably correlated with the structure and behavior of bulk samples. Similar experiments were done in the present work with rubidium and C222. Optical absorption spectra were obtained in 13 separate runs and four-probe conductivities were measured in 9 runs. The behavior was remarkably similar to that of $K^+(C222)e^-$, so much so that without labels one could not tell which of the metals had been used! For example, both the K and Rb systems give an initial absorption peak typical of M^- when the films are formed at low temperatures (−60 °C or colder). This probably results because of the slow encapsulation of M^+ by C222 and the thermodynamic stability of M^- relative to M^+ and e^-. The peak of Rb^- occurs at ∼900 nm. Upon long standing or warming to −40 °C the peak of Rb^- (or K^-) decreases and the IR peak of e^- increases, accompanied by the formation of considerable "plasma-like" absorption. Changes of this type were amply verified in the studies of $K^+(C222)e^-$ films. A further increase in temperature converted the "plasma-like" spectrum to a broad peak at ∼1380 nm with higher absorbance, characteristic of electrides with more localized electrons. These features are illustrated by the spectra shown in Figure 7. The same general behavior was observed with all four runs in which the films were formed below −50 °C, as was the case for 19 films of $K^+(C222)e^-$ studied previously.

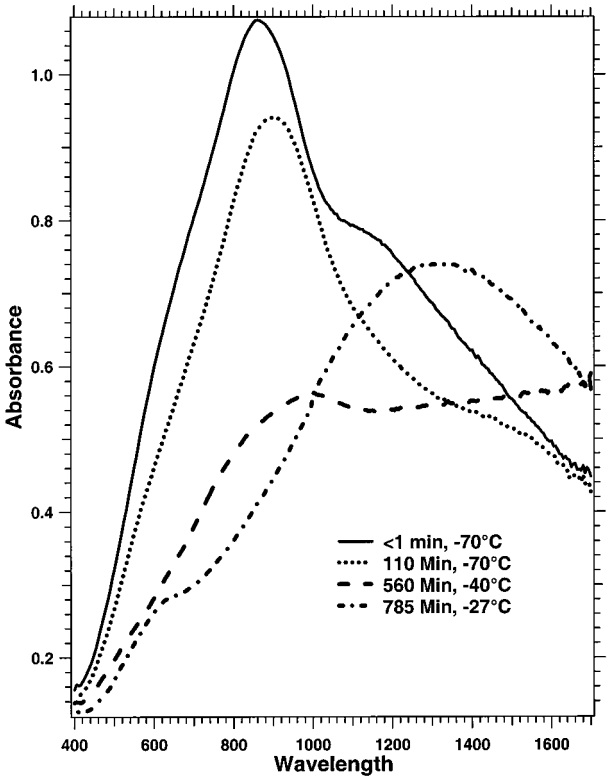

Figure 7. Spectra of a 2270 Å thick vacuum co-deposited film of $Rb^+(C222)e^-$. Deposition was carried out at a temperature of −70 °C. The peak at ∼900 nm is that of Rb^- which "anneals" at −40 °C to a "plasma-like" spectrum (dashed line). At higher temperatures this converts to a more "localized" peak at ∼1380 nm.

Table 2. Absorbance and Conductivity of Thin Films of $Rb^+(C222)e^-$ Formed at − 40 ± 2 °C

run date	thickness (Å)	initial abs	specific cond. ($ohm^{-1}\,cm^{-1}$) initial	later	time of later measmt (hs)	% dec. in abs
10/30/96	3190	0.845			2.3	3.3
11/07/96	3100	0.997	159	136	1.6	4.6
11/13/96	3100	0.928	83	118	1.4	2.3
01/28/97	2750	0.860	36	26	2.1	7.0
02/25/97	3140	0.949	41	57	1.0	2.5
03/31/97	4230	1.368	54	40	1.0	2.5
04/17/97	4180	1.157			1.9	3.3
04/23/97	4190	1.182	39	38	1.0	5.7
05/13/97	3361	0.956	31[a]	28	1.9	11.6

[a] After 0.93 h.

Deposition at about −40 °C usually produced little or no Rb^- absorption, similar to the generally small K^- absorption observed after co-deposition of K and C222 at this temperature. Apparently conversion of the alkalide to the electride occurs more rapidly at the higher temperature. After such deposition, for the Rb-C222 system, if the temperature was maintained constant, reduced to as low as −90 °C, or raised to as high as −15 °C, the peak position and shape remained essentially unchanged. The initial peak position for deposition at −40 ± 2 °C in nine separate runs was 1275 ± 7 nm. The decrease in the peak absorbance because of decomposition during the first 1−2 h after deposition ranged from 2.3% to 11.6%, with an average of 4.7%. The data for all nine runs at this temperature are given in Table 2. The first three spectra in Figure 8 are typical of the behavior of films deposited at −40 °C. Although they show the IR peak that is characteristic of localized electrons, there is

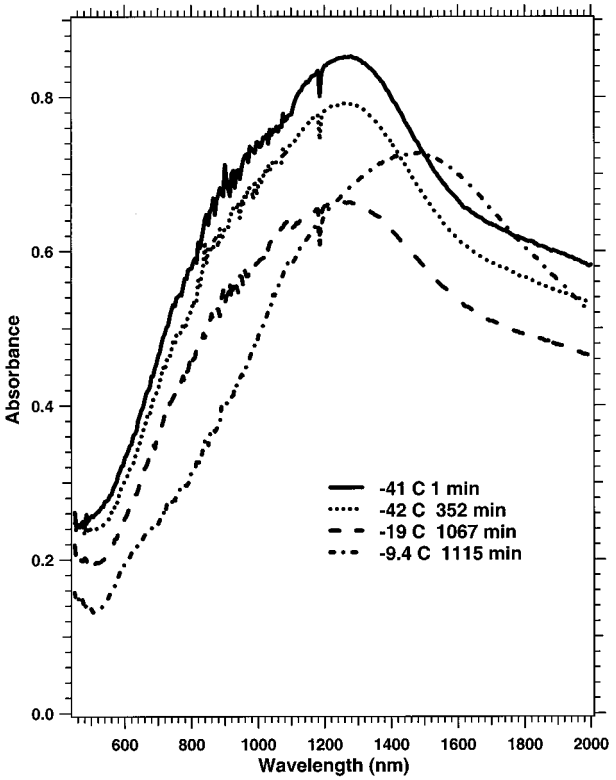

Figure 8. Spectra of a 3190 Å thick vacuum co-deposited film of $Rb^+(C222)e^-$. Deposition was at −41 °C. The top three spectra are similar with a "localized" peak at 1275 nm superimposed upon a "plasma-like" spectrum. An abrupt change to a more "localized" peak at 1500 nm occurs upon raising the temperature to −9.4 °C.

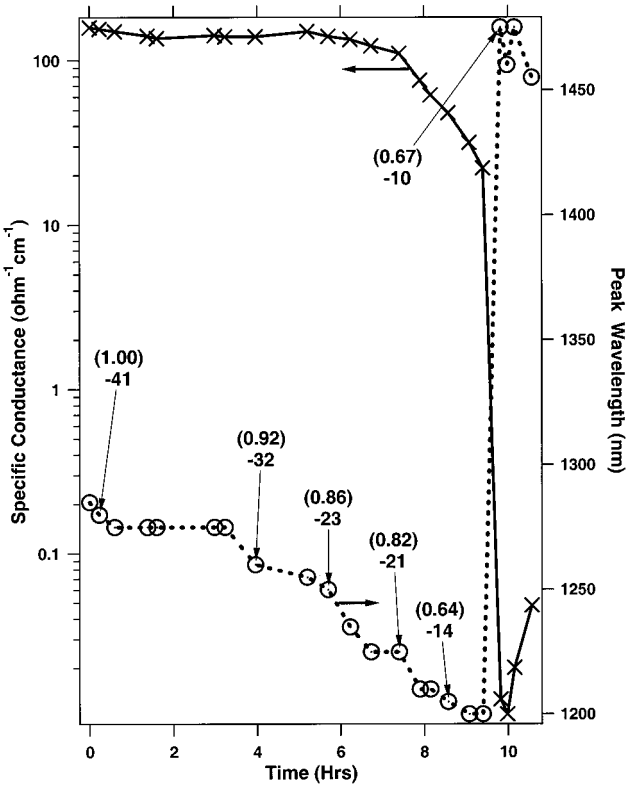

Figure 9. Variation with time and temperature of the four-probe specific conductance (×) peak wavelength (○) and peak absorbance of a 3100 Å thick vacuum co-deposited film of $Rb^+(C222)e^-$. The peak absorbance is given in parentheses and the film temperature (in °C) is also given. Note the abrupt changes that occur when the film temperature is increased to −10 °C.

also a substantial "plasma-like" contribution, as indicated by the tendency to reach a plateau at 2000 nm.

A striking and sudden shift in the peak position and absorbance occurred for films deposited at −40 °C when the temperature was increased to −12 °C or higher. The peak position shifted to 1500 ± 30 nm (five runs), usually accompanied by an *increase* in the peak absorbance. The final spectrum (at 1115 min) in Figure 8 is typical. Note the pronounced peak shift and absorbance increase when the film temperature was increased from −19 to −9.4 °C. The increase in absorbance occurs despite rather rapid decomposition at this temperature. The change is irreversible; reducing the temperature to −40 °C or below shortly after the transition had no effect on the spectrum. Another similarity of the $Rb^+(C222)e^-$ films to those of $K^+(C222)e^-$ is the high conductivity of the films. Films of $Cs^+(18C6)_2e^-$ and $K^+(C222)K^-$ are insulating, with $\sigma < 10^{-4}$ ohm^{-1} cm^{-1}. By contrast, films of both $K^+(C222)e^-$ and $Rb^+(C222)e^-$ are *much* more conducting, with four-probe specific conductances as high as 159 ohm^{-1} cm^{-1}. In the potassium case, both the magnitude of the specific conductance and its temperature dependence are similar to those of polycrystalline samples.[35,41] The high conductivity was ascribed to the very open cavity-channel geometry of this electride compared with all others of known structure.

As was the case with $K^+(C222)e^-$, the conductivity of co-deposited $Rb^+(C222)e^-$ films at temperatures below about −12 °C depended on the preparation, time, and temperature. Various films prepared at about −40 °C had initial four-probe specific conductances that ranged from a low of 31 ohm^{-1} cm^{-1} to a high of 159 ohm^{-1} cm^{-1}. During the first 1−2 h at constant temperature the conductivity was nearly constant (Table 2). The later trend with time as decomposition occurred was a decrease in conductivity. Data for seven films are given in Table 2. The conductivity of fresh films decreased with decreasing temperature, but it was difficult to separate the effects of time and temperature. The conductivities of two films formed below −60 °C were only slightly lower despite the presence of the Rb^- optical peak. Again, similar behavior had been seen in the K-C222 system.

As occurred with the optical spectra, increasing the temperature to −12 °C or above resulted in dramatic changes in the conductivity. The specific conductance dropped suddenly by at least 2 orders of magnitude. The time and temperature dependence of the specific conductance, the wavelength of the optical peak, and the peak absorbance are shown in Figure 9 for one of the films. All three properties change abruptly and irreversibly upon warming to −12 °C or above. The low conductivity of this phase suggests that it may result from the conversion of the "$K^+(C222)e^-$ like" phase β to the more insulating phase α. Similar behavior was found for the only film prepared at −64 °C that had been warmed to −12 °C.

Although it could be argued that the abrupt changes in the optical spectrum and conductivity are caused by decomposition rather than a phase transition, there are several reasons to reject this explanation. In all of our studies of alkalide and electride films, decomposed films show *no* optical peaks in this region of the spectrum, so it is very unlikely that the observed near-IR peak is that of a decomposed film. Furthermore, when films that have never been heated to the transition temperature are allowed to decompose, there is no peak shift; rather, the absorbance peak just decreases in intensity until it reaches the background level. As shown in Figure 8, the conversion actually occurs with an *increase* in peak absorbance. Upon further

standing, either above or below the transition temperature, the absorbance of converted films gradually decreases without any change in peak position until it reaches the baseline value. In contrast to the abrupt decrease in the specific conductance as soon as the temperature is increased to about −12 °C (see Figure 9), films kept below this temperature showed *gradual* decreases in conductivity as decomposition proceeded. After the transition, cooling samples to −40 °C (before substantial further decomposition) restored neither the optical spectrum nor the conductivity to the values that obtained before the transition. Of course, we cannot confirm that the transition is from phase β to phase α, but these observations strongly support a phase transition rather than decomposition alone.

Conclusions

The crystal structure of the α phase of $Rb^+(C222)e^-$ is different from that of any other electride, but the geometry of the cavity-channel system is similar to that of $Li^+(C211)e^-$. The predominant feature is a 1D zigzag collection of trapping sites connected by rather open channels. As with other electrides that have predominantly 1D channel-cavity geometry, the inter-electron coupling is in accord with the Heisenberg linear antiferromagnet model. The coupling constant agrees well with that expected from the channel size as shown in Figure 5. In addition, the conductivity of packed powders of phase α is low, as with other "localized" electrides.

The behavior of thin films produced by high-vacuum co-deposition of Rb and C222 is in marked contrast to that of bulk polycrystalline samples of phase α, but it is compatible with the behavior of phase β powders. Vapor-deposited films undergo a sudden irreversible change at about −12 °C to an insulating state with a "localized type" absorption spectrum. These changes occurred with all films that were brought to this temperature, regardless of the extent of previous decomposition. This indicates that the change is a phase transition rather than a general effect of decomposition. The simplest explanation is that the film structure changes from phase β, similar to that of $K^+(C222)e^-$ films, to that of phase α, an insulating film with a more localized optical spectrum.

The most plausible explanation of the differences between vapor-deposited films and bulk samples and of the differences between bulk samples of phases α and β is that $Rb^+(C222)e^-$ exists in two structural forms. According to this hypothesis, vapor co-deposited films tend to form with a structure similar to that of $K^+(C222)e^-$. Powders formed by slow evaporation of methylamine also yield primarily this phase. On the other hand, crystal-growing from mixed solvents gives a different structure and it is the only form of $Rb^+(C222)e^-$ whose structure could be directly determined. Numerous attempts were made to grow crystals at different temperatures and from other solvents and solvent mixtures in the hope that a second crystalline form could be isolated. All such attempts led only to samples with properties similar to those of phase α. Slow evaporation of methylamine from solutions in this single solvent gave powders with properties that are compatible with a $K^+(C222)e^-$-like structure. The solubility of $Rb^+(C222)e^-$ in methylamine is too high for the preparation of good crystals. The powders formed from solvent evaporation are unlikely to contain residual solvent, since they were evacuated to 10^{-5} Torr for extended periods of time before being harvested. We conclude that $Rb^+(C222)e^-$, as is the case for three other electrides, can exist in two forms, one of known structure, whose channel-cavity geometry is similar to that of $Li^+(C211)e^-$, and a second one whose properties suggest a structure similar to that of $K^+(C222)e^-$. However, without isolation of single crystals with the latter structure type, this interpretation remains speculative.

Acknowledgment. This research was supported by NSF grant No. DMR-96-10335 and by the Michigan State University Center for Fundamental Materials Research.

Supporting Information Available: Tables of atomic coordinates, bond distances and angles, and general thermal parameters for $Rb^+(C222)e^-$ (PDF), as well as X-ray crystallographic files (CIF). This material is available free of charge via the Internet at http://pubs.acs.org.

JA9943445